JOURNAL OF CATALYSIS 71, 175–191 (1981)

Model Studies on Bimetallic Cu/Ru Catalysts

III. Adsorption of Carbon Monoxide

J. C. VICKERMAN,[1] K. CHRISTMANN, AND G. ERTL

Institut für Physikalische Chemie, Universität München, D-8000 München 2, Sophienstrasse 11, West Germany

Received March 2, 1981; revised May 13, 1981

The adsorption of CO on Cu-covered Ru(0001) surfaces prepared at different temperatures was studied in UHV between 150 and 350 K by means of LEED, thermal desorption spectroscopy (TDS), and work function change ($\Delta\varphi$) measurements. Cu deposition at 540 K leads to statistically distributed nuclei which grow to three-dimensional clusters, deposition at 1080 K gives a more dispersed and strictly two-dimensional Cu atom distribution. The amount of strongly chemisorbed CO is greatly reduced by the presence of Cu, and the results indicate the clear operation of an ensemble effect with 3 Ru atoms participating in binding 1 CO molecule. A small ligand effect accounts for the slight reduction of the CO binding energy observed over the bimetallic surfaces. At ~150 K adsorption temperature, there is evidence that isolated copper atoms are capable of forming complexes of the kind $Cu(CO)_2$; in addition various low-energy Cu/Ru "mixed" sites become populated by CO. Moreover, the proximity of Ru atoms enables Cu atoms on top to adsorb CO more efficiently in that the well-known CO back-donation mechanism is allowed for by a transfer of charge from Ru to Cu atoms. The importance of the ensemble effect with respect to the adsorption mechanism (i.e., dissociative or nondissociative) is compared and discussed in view of recent adsorption studies on bimetallic Ru/Cu surfaces.

1. INTRODUCTION

In a recent series of papers (*1–3*) we showed that single-crystal systems consisting of a clean ruthenium (0001) surface covered with various amounts of copper provide fairly detailed insight into the microscopic operation of corresponding bimetallic cluster catalysts. Similar work has been performed by White and co-workers (*4*). Bimetallic Cu/Ru catalysts were introduced and investigated by Sinfelt *et al.* (*5, 6*) and were found to exhibit unique properties, in particular with respect to activity and selectivity in hydrogenolysis and dehydrogenation reactions. Our preceding study on the interaction of hydrogen with Cu/Ru single-crystal surfaces under UHV conditions (*3*) revealed striking similarities to Sinfelt's results in that it clearly demonstrated the inhibiting role of Cu atoms on the strong chemisorption of hydrogen. Similar work on the uptake of oxygen (either from O_2 or N_2O) was recently performed by Shi *et al.* (*4*).

The present work concerns the adsorption of CO on Cu/Ru surfaces, which was considered to be a suitable probe for characterizing the microscopic properties of these model systems. CO adsorbs quite strongly on Ru(0001)—the heat of adsorption was determined to be between 140 and 160 kJ/mole (*7*)—and it forms, depending on the coverage, various ordered phases with well-defined LEED patterns (*8*). According to Hollins and Pritchard (*9*), CO adsorbs on Cu(111) (whose face is formed by epitaxial growth of Cu on Ru(0001)) with a much lower binding energy, viz., only ~50 kJ/mole. It also forms various LEED superstructures on Cu(111), especially at higher coverages (*10*). From these properties it should be possible to differentiate between adsorption on Ru- and Cu-like (and eventually "mixed") surfaces sites.

[1] Permanent address: University of Manchester Institute of Science and Technology, P.O. Box 88, Manchester M 60 1 Q D, United Kingdom.

0021-9517/81/090175-17$02.00/0

Cu/Ru bimetallic catalysts might be of some importance for catalytic reactions involving CO, e.g., carbonylation or CO hydrogenation. By modifying the surface geometry and/or electronic structure (which can easily be done by varying the concentration and distribution of the surface copper) certain ranges of activity and selectivity can be achieved, particularly if hydrogen is used as a further reactant. Accordingly, several studies on the kinetics and mechanism of such reactions over bimetallic or supported Ru catalysts have been performed in the past, e.g., by Vannice (*11*), Dalla Betta (*12*), Bond and Turnham (*13*), and recently by Bossi *et al.* (*14*). The investigation by Bond and Turnham (*13*) revealed a fall in activity with Cu concentration which parallels our own observations on the uptake of chemisorbed hydrogen on Cu/Ru single-crystal surfaces. These data (*13*) suggested that ensembles of at least four neighboring Ru atoms were required to sustain activity. Related observations were made by Yu *et al.* (*15*) for CO interacting with Cu–Ni alloy surfaces, or by Burton *et al.* (*16*) for CO interacting with (111) faces of Au–Ni alloys, where $n = 3$ for the number of adjacent Ni atoms required to strongly adsorb CO was derived. Ag/Pd single-crystal alloy surfaces revealed $n = 3.5$ for the same molecule (*17*). From all of these studies it appears that certainly more than just one surface atom is involved in binding a single CO molecule, a phenomenon first referred to as "ensemble effect" by Sachtler (*18*). The basic ideas, however, have been pointed out as early as 1929 by Balandin in his multiplet theory (*19, 20*). In order to study the ensemble effect in detail the Cu/Ru system is clearly attractive in that it consists of one strongly bonding (Ru) and one weakly bonding (Cu) component.

Besides the ensemble effect the present study highlights the question of how a clean homogeneous metal surface is modified with respect to both surface geometry and electronic structure if a second component like Cu is deposited. Depending on their binding site and degree of dispersion more than a single ligand may be attached to a Cu atom; observations of this kind have recently been made with rhodium (*22*), and copper carbonyls of the type $Cu(CO)_2$, $Cu(CO)_3$, or $Cu_2(CO)_6$ are known from matrix isolation studies (*23*).

In this paper results of CO adsorption on a high- and low-temperature deposition series of Cu on Ru(0001) are described. A later paper will deal with coadsorption of CO and D_2 on the same surfaces. Details of the preparation of the Cu films on Ru(0001) were reported previously (*1, 2*), results of a recent investigation (using among others synchrotron radiation) of the geometric and electronic structure of the Cu film surface will be published elsewhere (*21*).

2. EXPERIMENTAL

The experiments were performed in a Varian UHV system with a base pressure of about 10^{-8} Pa. The apparatus contained facilities for LEED, Auger electron spectroscopy (AES), using a cylindrical mirror analyzer; temperature-programmed thermal desorption (TDS), using a quadrupole mass analyzer (Balzers), and work function measurements ($\Delta\varphi$), employing a Kelvin vibrating capacitor with an inert tantalum oxide reference electrode.

The oriented and mechanically polished Ru(0001) sample was mounted between two 0.2-mm molybdenum wires that were attached to the sample manipulator. The crystal temperature could be varied and controlled between 120 and 1500 K using a combination of a programmable dc power supply (*24*) and a modified Varian liquid N_2 cooling device. The sample temperature was monitored by a chromel–alumel thermocouple spot-welded to the rear of the crystal. High-purity CO (99.99%, Messer-Griesheim) could be admitted to the system via a high-precision bakeable leak valve (Varian).

Following the procedure of Madey *et al.* (*25*), the Ru surface was cleaned by a series of oxidation/reduction cycles with oxygen

and hydrogen followed by mild argon ion sputtering and subsequent rapid annealing to 1500 K. This procedure was effective in removing all contaminants detectable by AES. It was, however, impossible to judge the concentration of carbon by AES due to the overlap of the C 275-eV peak and the strong Ru 281-eV Auger transition. In contrast to the observations reported by Goodman and White (*26*), the analysis of the region 250–265 eV with respect to carbidic carbon AES peaks was found not to reliably reflect small concentrations of C impurities. The only satisfactory methods for determining whether the surface was carbon free consisted in monitoring the work function of the Ru surface relative to the Ta reference electrode, or (as has been suggested elsewhere (*3*)) to monitor the effect of H adsorption on the Ru work function.

Evaporation of Cu onto the Ru surface was achieved by an electronically regulated evaporation source (*27*). Two series of bimetallic surfaces were studied: The first one was obtained by condensing Cu vapor on the Ru surface kept at 540 K, the other series was prepared in an analogous manner except that the crystal was held at 1080 K during Cu deposition and then rapidly cooled to 320 K. Without entering into any detail of the characterization of the Cu films, which is given elsewhere (*21*), it has to be noted that the different deposition temperature had a strong effect on the Cu growth mechanism and thus on the topography of the bimetallic surfaces. For the 540-K series, basically a Stranski–Krastanov growth mechanism seems to describe the situation rather well; i.e., three-dimensional Cu islands are formed on top of a first Cu monolayer. There is, however, some evidence that this first monolayer is not completely built up before the three-dimensional cluster growth occurs (*2*). For the 1080-K series another mechanism, namely, the Frank–van der Merwe type, with layer-by-layer growth holds. In this case, also, the structure of the first monolayer of Cu is more perfect. It should be mentioned that the temperature-dependent Cu growth features just described are in close agreement with Sinfelt's results on bimetallic Cu/Ru cluster catalysts, in which after the use of higher preparation temperatures a pronounced tendency to form two-dimensional Cu monolayers was observed (*28*).

It is difficult to precisely characterize the structure of the *submonolayer* surface copper. The adsorption results indicate that the temperature of the Ru substrate during Cu deposition also governs the *distribution* of the Cu atoms in the submonolayer concentration range to a large extent: If the deposition temperature is low, a given amount of Cu tends to form three-dimensional islands (thereby also creating a considerable surface roughness), whereas at the higher deposition temperature increased thermal mobility allows more uniform spreading of the Cu atoms over the substrate surface.

3. RESULTS

Although the adsorption systems CO/Ru(0001) and CO/Cu(111) have already been extensively investigated in the past, in particular, by Menzel, Madey and co-workers (*7*, *29–31*), and by Pritchard *et al.* (*9*, *10*, *32*), respectively, it was necessary to reproduce some of these data first in order to get a proper basis for an *in situ* comparison between the clean and the Cu-covered ruthenium surfaces.

Without entering into a detailed description of these results some of our (sort of boundary) data for CO on Ru(0001) and Cu(111) are included in the respective figures illustrating the properties of the bimetallic surfaces. We only state here that our CO adsorption data on Ru(0001) and Cu(111) agree quite well with those published previously in the literature.

The results reported next will be subdivided into high- and low-temperature CO adsorption experiments in order to clearly separate the "strong" CO chemisorption from the more weakly held carbon monoxide. Where it is necessary, we also distinguish the CO adsorption on Cu/Ru surfaces

prepared at 540 K (the "540-K series") and at 1080 K (the "1080-K series"), in order to shed light on the influence of the dispersion of the submonolayer copper on the CO adsorption.

3.1. Bimetallic Surfaces—CO Adsorption at 320 K

All bimetallic surfaces were analyzed with respect to their surface composition by means of combined Auger and thermal desorption measurements as described elsewhere (*1, 2*). Throughout this paper, each bimetallic surface will be characterized by a number "y" which simply is the ratio between the Auger signal heights of the Cu $M_{2,3}M_4M_4$ 62-eV and the Ru $M_5N_{4,5}N_{4,5}$ 281-eV transition. It has to be noted that conversion of these Cu/Ru ratios into absolute or relative copper surface coverages, θ_{Cu}, depends on the dispersion of the Cu atoms on the surface, i.e. whether they exist in two-dimensional islands only or are also present in the form of three-dimensional clusters (a Cu coverage of 1 is defined as a close-packed hexagonal Cu layer containing 1.77×10^{15} atoms/cm^2). A direct $y \rightarrow \theta_{Cu}$ conversion is therefore only possible for the 1080-K deposition series which is thus more precisely defined than the 540-K deposition series.

(*a*) *LEED*

Our LEED observations at 320-K CO adsorption temperature are summarized in Table 1; they apparently do not provide any evidence for specific CO superstructures on the bimetallic surfaces. Instead all the observed patterns $(n3^{1/2} \times n3^{1/2})R30°$ with n = 1, 2, and 5 are also observed with pure Ru(0001) (*8*); however, from the appearance and suppression, respectively, of the high CO coverage patterns ($n > 1$) some information on the degree of copper dispersion and its inhibiting effect on the long-range order of the adsorbed CO can be gained which is in complete accordance with the findings reported in the following sections.

TABLE 1

Summary of the LEED Features Observed on Both the 540-K and the 1080-K Cu Deposition Series, If CO is Adsorbed at 320 K

I_{Cu}/I_{Ru}	Range of exposures for $(3^{1/2} \times 3^{1/2})R30°$	"Precursor" of $(2(3^{1/2}) \times 2(3^{1/2}))R30°$
Ru	1—3*L*	10*L*
	540 K	
0.06	0.5–1.5*L*	10*L*
0.11	0.5–1.5*L*	10*L*
0.25	0.5–0.8*L*	Absent
0.34	Diffuse background	Absent
0.52	Diffuse background	Absent
	1080 K	
0.06	0.5–1.5*L*	5*L*
0.17	0.3–0.5	3*L*
0.42	0.5–0.6	Very weak 8*L*
0.67	0.8–1.4	Absent

(*b*) *Thermal Desorption Spectroscopy*

The thermal desorption yields twofold information:

(i) From the shape and the position of the maxima of a thermal desorption trace the activation energy for desorption E^*_{des}, the frequency factor, ν, and the reaction order for desorption of the respective binding states of the adsorbate can be determined (*33, 34*), which allows conclusions to be drawn about, for example, the role of the ligand effect.

(ii) Other information is provided by the total desorption peak area $\int pdt$ and reflects the total amount of adsorbed gas; it can be evaluated as a function of the Cu concentration or be compared with the initially exposed amount of CO to give the relative or (less accurate) the absolute sticking probability s.

Interesting differences between the low-temperature (540 K) and the high-temperature (1080 K) deposition series become apparent in the thermal desorption experiments (heating rate 9 K sec^{-1}). The situa-

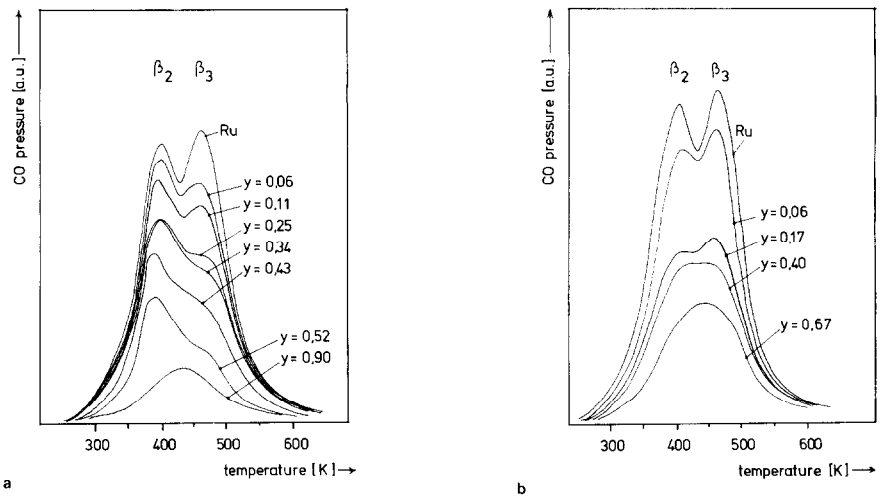

FIG. 1. (a) Series of thermal desorption curves corresponding to CO saturation at 320 K of the pure Ru(0001) surface and of various bimetallic surfaces (prepared at 540 K) ranging from $y = 0.06$ to $y = 0.9$. (b) Series of thermal desorption curves obtained under the same conditions except for a different Cu deposition temperature, which was 1080 K in this case.

tion is illustrated in Fig. 1, which displays TDS data obtained after CO saturation at 320 K from surfaces with varying Cu concentration ($\theta_{Cu} = 0.06$ to about 0.8). This figure also shows the CO desorption from a pure Ru(0001) surface which gives rise to a β_2 and a β_3 state as was reported by Pfnür *et al.* (*30*). In the 540-K series (Fig. 1a), the first small amounts of copper obviously depress the Ru β_2 state, but subsequent additions have a more dramatic effect in reducing the high-temperature β_3 state with the β_2 state remaining nearly unaffected. The 1080-K series (Fig. 1b) shows a different behavior: Cu additions seem to more or less equally affect both states and beyond $\theta_{Cu} = 0.12$ the two states can no longer be resolved. If we tentatively correlate the β_3 state with CO on "on top" sites and β_2 with CO on "in between" sites, then a statistical atomic distribution of Cu on the Ru surface should tend to affect both states roughly equally, possibly suppressing β_2 a little more than β_3, if β_2 results from CO ordering. This is in fact observed on the high-temperature samples. For the 540-K series the geometrically defined β_3 sites apparently are suppressed relative to the β_2 state which would imply that the clusters formed under these conditions will preferentially block the CO "on top" adsorption sites.

Figure 2a shows how the saturation coverage of CO (as determined by a numerical integration of the desorption traces), relative to clean Ru, varies with the Cu/Ru ratio for the two series. The qualitative behavior is obviously rather similar in both cases. It has to be remembered, however, that the Cu coverage scale is only accurate for the 1080-K series. A very strong decrease of the adsorbed amount of CO is apparent as the Cu coverage increases. This effect is more pronounced for the 1080-K series, and at $\theta_{Cu} = 1$ obviously no strongly held CO species is present any longer. In contrast to this, a y ratio of more than 1.0 is required for the 540-K series to reach zero CO coverage. This behavior indicates island growth of Cu in the latter case with the consequence that the same amount of Cu which completely covers the Ru surface in the 1080-K series still leaves "empty" Ru patches in the 540-K case that are able to adsorb CO.

According to Yu *et al.* (*15*), a log–log plot of the CO saturation coverage against the Cu monolayer concentration should reveal a straight line with slope n, where n equals

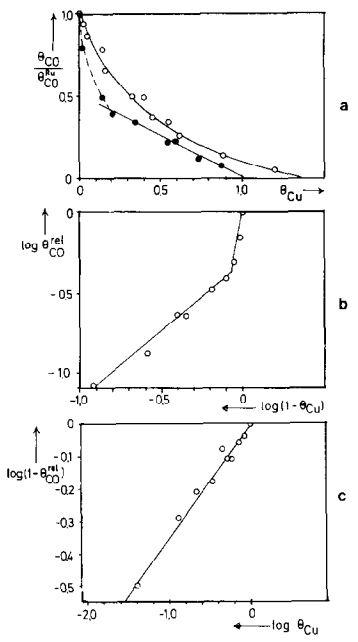

FIG. 2. (a) Variation of the normalized CO saturation coverage versus the copper surface concentration. Filled circles: 1080-K Cu deposition series; open circles: 540-K Cu deposition series. (b) Plot of log θ_{CO} (rel) versus log$(1 - \theta_{Cu})$ for the 1080-K Cu deposition series (see text for details). (c) log–log plot of the loss of CO coverage; i.e., log$(1 - \theta_{CO}(rel))$ versus the Cu surface concentration, log θ_{Cu}, for the 1080-K Cu deposition series.

the number of active surface atoms required to adsorb 1 CO molecule. This treatment implies a completely random distribution of the Cu atoms and also neglects short- or long-range order effects. That, however, those effects can change the simple pattern markedly is evident from Fig. 2b, where we tried a log–log plot of the CO coverage versus the active Ru surface $(1 - \theta_{Cu})$ for the 1080-K series. Apparently, there is a very steep decrease of the CO coverage as soon as a few Cu atoms are added; after θ_{Ru} drops below 0.79 the slope of the straight line changes from 5–6 to about 1.2 for all other Cu coverages. It is believed that this change is caused by a breakdown of the CO compression structure which needs short-range interaction *and* long-range interaction, and very few Cu atoms can break up large areas of Ru atoms required to form the compressed high-coverage CO patches. At higher Cu coverages merely one Ru surface atom is required to bond one CO molecule indicating a more or less "terminal" type of CO binding site. The phenomenon may be considered from the opposite viewpoint: As θ_{cu} falls, the CO coverage rises steadily until the removal of the last Cu atoms from the Ru surface suddenly allows the formation of higher local CO coverages, which then give rise to a strong final increase in the total CO coverage.

A different behavior is observed for the 540-K series, where a log plot reveals an initial decrease of the relative CO coverage with Cu addition of $n = 2.5$. This indicates clearly that for the same apparent surface concentration as measured by AES the fraction of the Ru surface effectively covered by Cu atoms is a factor of about 2 smaller than for the 1080-K series. Higher Cu coverages (i.e., $\theta_{Cu} \approx 0.6$) yield a slope of $n = 1.5$, very similar to the 1080-K series. Thus within the limitations imposed by the AES calibration for the 540 K series a very similar binding mechanism is indicated. It is instructive to extract the actual *loss* of CO binding sites produced by the addition of copper by plotting the logarithm of the loss of the CO coverage as compared to the clean Ru surface versus the logarithm of the Cu concentration for the 1080-K series (Fig. 2c). Interestingly, the data points can be fitted quite nicely by a straight line with slope 0.36 which simply means that each Cu atom added prevents the adsorption of three CO molecules. The same plot for the 540-K series cannot be interpreted so easily due to the uncertainty in θ_{Cu}, but in this case a slope of 1.0 is obtained which seems to indicate three-dimensional clustering of Cu atoms even at rather low overall concentrations.

With regard to the binding energy of the CO adsorbed on bimetallic surfaces it is clear from Fig. 1 that at most only a small shift of the characteristic CO/Ru β_2 and β_3 desorption state maxima occurs in a way

that higher Cu concentrations slightly lower the binding energy for CO on Ru sites. By varying the heating rate dT/dt, the activation energy of desorption (which in this case of nonactivated adsorption equals the CO binding energy) for a first-order process is accessible as already pointed out. With the 1080-K deposition series, average E^*_{des} values for the β_2 state between 166 kJ/mole for low and 159 kJ/mole for high Cu coverages result along with preexponential factors that range from $10^{18}sec^{-1}$ to $10^{15}sec^{-1}$.

Another point of interest that can be tackled by thermal desorption experiments is the kinetics of adsorption, i.e., the effect of the Cu addition on the sticking probability. Figure 3 shows how the initial sticking probability varies with the copper concentration on the Ru surface for the 1080-K deposition series. Surprisingly, there is an increase of s_0 by roughly 50% in going from a clean Ru surface to $\theta_{Cu} = 0.1$, followed by a decrease to the initial value of about 0.15 which remains constant up to $\theta_{Cu} = 0.6$. Basicly the same behavior is found with the 540-K deposition series except that the peak in the s_0–θ_{Cu} relation is somewhat higher than in the 1080-K series. It should be mentioned in this context that a similar (but less pronounced) increase of the sticking coefficient was observed with the pure Ru surface with variation of the CO coverage.

(c) Work Function

The deposition of Cu on the Ru surface radically alters the coverage dependence of the CO-induced work function change which for the clean (0001) face was found to initially rise linearly up to a maximum of 650 meV (7). In general, the linear relation between θ_{CO} and $\Delta\varphi$ is lost as soon as Cu is added, regardless of the Cu deposition temperature, and the work function initially rises more slowly with increasing CO surface concentration with the slope depending on Cu surface coverage.

If we wish to relate work function changes on the bimetallic surfaces to absolute CO coverages, it is not possible to use the intensity maximum of the CO-induced $(3^{1/2} \times 3^{1/2})R30°$ LEED pattern as a measure of 0.33 coverage as is the case on the clean homogeneous Cu(111) or Ru(0001) surfaces. We can, however, monitor the change in relative CO coverage across the series using the TDS data, and hence it is possible to observe the work function change for the adsorption of a given relative coverage of CO as a function of Cu surface coverage. Figure 4 shows the variation of $\Delta\varphi$ for a relative CO coverage of 0.17 (i.e., relative to θ_{max}(320 K) on Ru(0001)) as a function of θ_{Cu} for the two series of surfaces. It can be seen that there is a sharp fall in $\Delta\varphi$ and hence presumably in charge transfer to the adsorbing CO in the region of $\theta_{Cu} \sim 0.1$. The fall is apparently sharper

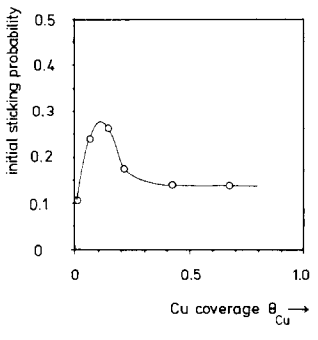

FIG. 3. Variation of the initial sticking probability for CO, s_0, versus the copper surface coverage (Cu deposition temperature 1080 K).

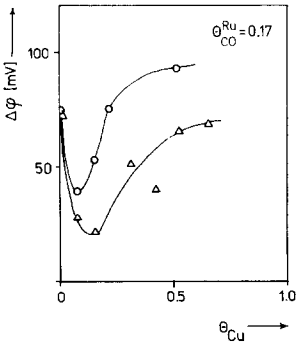

FIG. 4. Variation of $\Delta\varphi$ for a relative CO coverage of 0.17 as a function of θ_{Cu} for the 540-K (triangles) and the 1080-K series (circles).

for the 540-K series. Interestingly this fall correlates closely with the increased sticking coefficient, and, as later data will show, with the possible involvement of Cu in the adsorption process.

CO-induced work function changes were used as a coverage monitor to obtain adsorption isobars and hence to study the energetics of adsorption on Cu(111) and Ru(0001). The data shown in Fig. 5 is in good agreement with that obtained elsewhere (*9, 30*). The use of this technique on the bimetallic surface raises one area of uncertainty. We can and have characterized the variation of $\Delta\varphi$ with θ_{CO} at constant temperature, we have shown that the temperature variation of the work function of the bimetallic surfaces in the absence of CO is very small, but we do not know what the effect of temperature will be on their surface properties *in the presence of CO* and consequently how the overall work function changes may be influenced. Despite this uncertainty the isosteric heats were determined for the 1080-K series having low copper coverages (y = 0.06, 0.12, 0.17). These are also shown in Fig. 5. A fall in surface binding energy is observed which is in close agreement with the thermal desorption data, where a decrease in the activation energy for desorption correlated with a dramatic suppression of strongly held CO. The good agreement between the thermal desorption energies and the isosteric heats suggests that the uncertainty associated with possible temperature effects on the $\Delta\varphi$ of the bimetallics in the presence of CO is small.

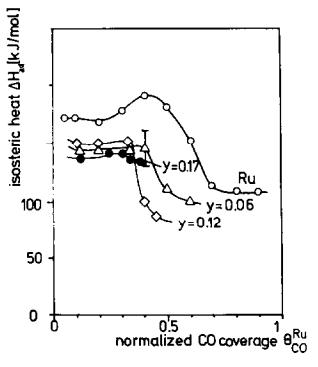

FIG. 5. Variation of the isosteric heat of CO adsorption as determined by work function measurements versus the relative CO coverage, parameter is the Cu concentration of the bimetallic surfaces prepared at 1080 K. Indicated in this figure is also ΔH_{iso} for the pure Ru(0001) surface.

Examination of Fig. 5 indicates that as θ_{Cu} rises a point is reached where the isosteric heat does not fall with θ_{CO}. This suggests that the formation of a compression structure is almost completely inhibited by the presence of Cu. Significantly this point ($\theta_{Cu} \sim 0.2$) correlates exactly with the end of the steep fall in CO coverage consequent on the first additions of Cu to the surface (Fig. 2a). Altogether, addition of Cu obviously strongly decreases the number of CO molecules adsorbed with the energy characteristic for the clean Ru surface and produces sites with a slightly lower binding energy (150 kJ/mole), owing to the operation of a ligand effect.

3.2. Bimetallic Surfaces—CO Adsorption at 150 K

We first recall that CO adsorption performed at temperatures as low as 150 K probes both the high-adsorption energy part associated with the Ru and the low-adsorption energy part associated with Cu and mixed Cu + Ru sites. The correct interpretation of the experimental data, in particular the thermal desorption data, is more difficult in this case, owing to the fact that at low adsorption temperatures even the rear side of the Ru crystal or parts of the sample manipulator may become capable of adsorbing CO which is released in a thermal desorption experiment and forms a nonuniform CO background pressure rise. Although we tried to eliminate this effect by covering the front side of the sample with a thick Cu film and, after subtracting the adsorbed amount of CO on copper from the overall desorption contribution, attributing the remainder to adsorption on rear side or manipulator areas, particularly the low CO coverage or exposure thermal desorption

data may be somewhat erroneous. There is, however, quite an elegant way to overcome this problem by following the work function change during a thermal desorption experiment (a method developed by Menzel and his group [36]) and by differentiating the $\Delta\varphi$ signal with respect to the temperature. Here, only the contribution from the front side of the sample crystal is measured, and there is also another advantage of this method that allows us to distinguish between CO molecules adsorbed on copper (which in general produce a work function decrease) and those adsorbed on ruthenium (which cause a work function increase), as will be shown further below.

(a) LEED—Cu Deposited at 1080 K

The principal difficulty with LEED is that a $(3^{1/2} \times 3^{1/2})R30°$ structure is formed by a third of a monolayer CO on both Cu and Ru which makes it impossible to distinguish between CO adsorbed on Cu and CO adsorbed on Ru from LEED observations alone. As was already pointed out in Section 3.1(a), the degree of information we obtain from the LEED experiments is rather limited: As in the 320-K adsorption data there is no novel CO LEED structure formed under the low-temperature conditions; sometimes superpositions of CO patterns found with pure Ru(0001) occur. The LEED results for 150-K adsorption temperature are summarized in Table 2. As a matter of fact the CO-induced diffraction features that occur in the low Cu concentration range all arise from occupation of empty Ru areas of the bimetallic surface. Molecules attached to the randomly distributed Cu atom sites contribute only to the

TABLE 2

Summary of the CO-Induced LEED Features on Bimetallic Surfaces Prepared at 1080 K, CO Adsorption Performed at 150 K

I_{Cu}/I_{Ru}	$(3^{1/2} \times 3^{1/2})R30°$	Range of exposures for observation of		
		Intermediate pattern (*8*)	$(2(3^{1/2}) \times 2(3^{1/2}))R30°$	Compression pattern (*8*)
Ru	0.5*L*	?	2.5*L*	>10*L*
0.08	1–1.5*L*		~5*L*	>15*L*
0.12	1–1.5*L*			
0.08 + 0.15 warmed to 200 K		Superposition of "intermediate" pattern [8] and "$2(3^{1/2})$ pattern"		
0.25 – 0.6	1–1.5*L*	2.5*L*	>10*L*	Not observed
0.8	1–1.5*L* + diffuse background		>5*L*	Not observed
0.8	1–1.5*L* + strong diffuse background		>5*L*	Not observed
1.8	1–1.5*L*		>10*L*: CO compression pattern with split spots as it is observed on pure Cu(111)	
20	~1*L*		Complex pattern (3 domain $c(4 \times 2)$ structure)	

diffuse background scattering. We also note that even small amounts of Cu prevent the formation of the high-coverage CO compression structures observed with pure Ru, a feature which was also concluded (in a much more direct manner) from the thermal desorption data to be reported next. At high Cu coverages the $(3^{1/2} \times 3^{1/2})R30°$ structure typical for CO/Cu(111) becomes visible indicating CO adsorption on the epitaxially grown Cu(111) film.

(*b*) *Thermal Desorption Spectroscopy (TDS)*

Nine surfaces prepared at 1080 K with copper concentrations varying from θ_{Cu} = 0.02 to 2.0 monolayers were studied. Figure 6 shows a series of thermal desorption spectra obtained after saturation of the adlayer at 150 K. If compared with the spectra shown in Fig. 1 it becomes clear that in addition to the "Ru" CO TD peaks at 406 and 478 K there appear new desorption states below 300 K. These are not present on a clean Ru surface and must be a consequence of the Cu on the surface. (A pronounced tail on the low-temperature side of the CO/Ru(0001) TD spectra is not a CO desorption state but is due to contributions from the sample holder and the rear of the samples and is omitted in our Fig. 5). It was, however, quite difficult to determine the background contribution for the desorption from the bimetallic surfaces which therefore have not been corrected in this figure and may still contain a (fairly uniform) background signal. The Ru β_2 and β_3 states around 400 and 480 K are easily identified, their maximum temperatures are almost not affected by the presence of Cu. With increasing Cu concentration these β_2 and β_3 states get weaker and blurred and can no longer be separated for Cu coverages above θ = 0.25. A high-temperature desorption state persists as a very broad peak, possibly superimposed by desorption contributions from mixed Cu–Ru sites.

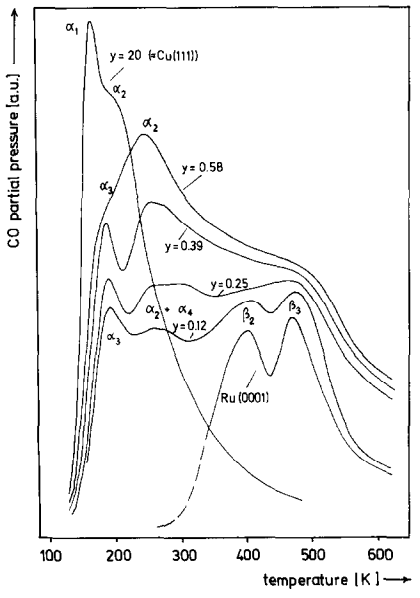

FIG. 6. Series of thermal desorption curves for the "1080-K series" with CO adsorbed to saturation at 150 K. Included for comparison are also the corresponding curves for the pure Ru(0001) and Cu(111) surfaces, respectively. The various desorption states are indicated. The heating rate was 5 ksec^{-1} in this case.

The low-temperature desorption states tend to run together and can be difficult to clearly distinguish with TDS. Variation of the rate of heating does enable us to distinguish three and possibly four states, designated α_1, α_2, α_3, and α_4. Examination of these four states as a function of θ_{Cu} and in conjunction with the work function measurements reported in the next section suggest that α_1 and α_2 are associated with CO adsorption on Cu clusters or bulk Cu. α_2 occurs in the region 200–240 K, and as the Cu layer becomes continuous its T_{max} shifts back toward 200 K. α_1 is found only at high CO coverages on highly ordered Cu surfaces in the region 150–180 K and seems to be associated with the CO which forms the compression structures on Cu(111) and results in a positive work function change. α_3 appears particularly at low θ_{Cu} in the region 200–220 K and may be associated with adsorption on "single" Cu atoms. α_4 found in the region 300–330 K is observed below $\theta_{Cu} \sim 0.7$, and can be argued to arise from mixed Cu–Ru sites.

A full quantitative analysis of the desorption curves with respect to E^*_{des}, ν, and θ_{max} was not found to be useful due to problems of deconvolution and uncertainty as to the corrections required for adsorption on the rear and edges of the crystal. Some rough estimates of E^*_{des} were made using the Redhead formula based on the variation of the heating rate (*33*)—values of around 40–60 kJ/mole were obtained for α_1, and 65–85 kJ/mole for α_2, respectively. Figure 6 also shows the CO saturation desorption curve from a 20-layer Cu(111) film, where two maxima occur, one around 160–180 K, which is identified as CO α_1 state, and one at about 200–220 K, the α_2 state. Since some of the α_1 population is already pumped off before the TD experiment is performed, the maximum temperature is likely to appear at too high a temperature.

Despite the uncertainty in the absolute determination of the aforementioned desorption parameters it was nevertheless possible to assess the effect of Cu on the total CO coverage (corrected for edge and rear contributions) after saturation exposure at 150 K: Fig. 7 shows the variation of the total CO coverage and also of the CO coverage above 320 K (obtained under saturation conditions) as a function of the copper surface concentration θ_{Cu}, with θ_{CO} normalized with respect to the full coverage on clean Ru at 320 K (which was $\theta_{CO} \sim 0.50$). Interestingly, at $\theta_{Cu} = 0.1$ the CO saturation coverage at 120 K peaks sharply and is nearly twice as large as on pure Ru. At higher Cu concentrations the amount of adsorbed CO decreases and reaches the (about equal) uptake of the clean Ru or Cu surfaces. Although Ru atoms are covered with Cu and thereby lost as strong CO adsorption sites it becomes clear from this observation that new sites are formed in equal or even higher concentrations (however, with a lower CO binding energy) consisting of either Cu atoms or mixed Cu/Ru atom ensembles.

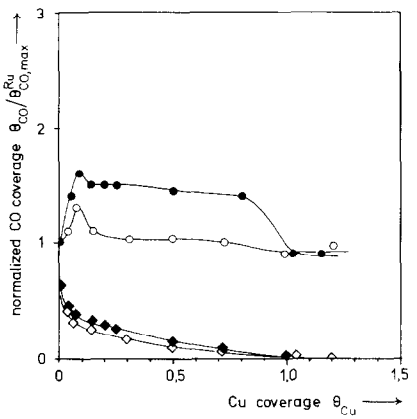

FIG. 7. Variation of the relative adsorbed amount of CO, normalized to the saturation CO coverage of the pure Ru(0001) surface at T = 150 K, as a function of the Cu surface concentration. The full symbols represent the 540-K, the open symbols the 1080-K deposition series. Shown in the bottom of the figure for comparison is also the corresponding CO uptake at room temperature.

Less detailed measurements were performed with samples prepared at 540 K. CO was always adsorbed to saturation at T_{ad} = 150 K. All the desorption states mentioned above were observed here, too. Some of the peaks are more readily distinguished using temperature-programmed work function measurements. Evidently, the α states grow rapidly with increasing Cu coverage. A plot of the maximum θ_{CO} versus θ_{Cu} is also included in Fig. 7; it reveals an even more pronounced increase of the CO saturation coverage than the 1080-K deposition series. As before, the total CO coverage reaches a maximum value near $\theta_{Cu} = 0.1$ monolayers. The low-temperature component of the adsorbed CO (i.e., that below 300 K) then is relatively constant up to $\theta_{Cu} = 0.7$, where it sharply drops to the value associated with the clean Cu(111) surface. It is noteworthy that at this Cu coverage the two-dimensional growth is nearly completed and the three-dimensional growth begins. The difference in CO adsorption capacity between the 540-K and the 1080-K series around $\theta_{Cu} = 0.1$ may be due to an increased atomic roughness of the 540-K surface. As the Cu coverage increases the surface again gets smoother.

(c) Work Function Measurements

Two types of measurements are reported here: First, the change of the work function of a surface was monitored as a function of CO exposure, CO pressure, and of the Ru/Cu–Ru surface temperature. Second, the change of the work function was followed during a thermal-desorption experiment.

As far as the work function change–exposure relation is concerned, we observe an even stronger reduction of the positive $\Delta\varphi$ contribution associated with adsorption on Ru sites than was observed in the 320-K adsorption experiments; for $\theta_{Cu} = 0.7$ the positive and negative part of the work function change almost cancel each other, and for even higher Cu concentrations an overall work function *decrease* is found. This clearly demonstrates that CO adsorption increasingly takes place on Cu or Cu-like chemisorption sites, it is, however, quite difficult at this stage to delineate completely between CO adsorbed on Cu and that adsorbed on Ru sites.

By following $\Delta\varphi(T)$ we may be able to distinguish CO released from Cu or Cu-like sites and CO desorbed from Ru or Ru-like adsorption sites. The reason lies simply in the pronounced difference of the adsorption enthalpy for CO on Cu and for CO on Ru as became evident from the TDS data. Figure 8 shows a series of "$\Delta\varphi$-TD" curves (broken lines) where roughly a 100-K separation between the main Cu–CO and the main Ru–CO desorption peaks can be seen. A correlation of the sign and magnitude of an observed work function change with the corresponding adsorption or desorption state, however, may not be so easy but can be clarified by differentiating the $\Delta\varphi$ with respect to the temperature rise to yield a type of desorption spectrum.

In detail, Fig. 8 shows both $\Delta\varphi(T)$ and $d\Delta\varphi/dt(T)$ for clean Ru(0001), for clean Cu(111) (a 20-layer epitaxial film) and for three bimetallic surfaces with Cu concentrations of $\theta_{Cu} = 0.15$, 0.7, and 1.0; the Cu

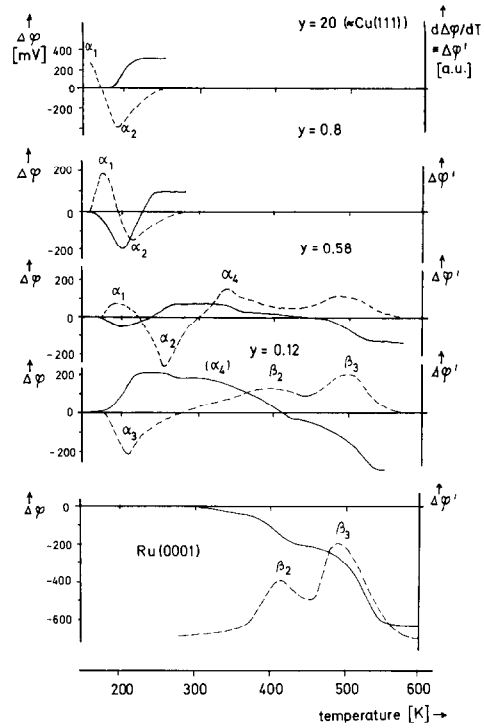

FIG. 8. Temperature dependence of the CO-induced work function change $\Delta\varphi_{CO}(T)$ (full lines) and its temperature derivative $d\Delta\varphi/dT$ (dotted lines) for pure Ru(0001), pure Cu(111), and for three bimetallic surfaces ($y = 0{,}12, y = 0{,}58, y = 0{,}8$) prepared at 1080 K. The CO adsorption temperature was 150 K throughout. The various α and β adsorption states are indicated.

deposition temperature was 1080 K. With the pure Ru(0001) surface, the CO β_2 and β_3 states are clearly distinguished from the $d\Delta\varphi/dT$ curve and no low-temperature states show up as is expected. Low concentrations of copper ($y = 0.03$–0.25) cause the CO/Ru $\beta_2 + \beta_3$ states to decrease in intensity, again evident from the $d\Delta\varphi/dT$ data, and, in addition, give rise to the development of a broad desorption feature with the maximum desorption temperature around 210 K. As this state (which corresponds to the aforementioned α_3-state) desorbs, the work function of the sample increases which means that the α_3 state itself causes a work function decrease.

It is significant that this state is clearly evident in the 1080-K series up to $\theta_{Cu} \sim 0.3$,

whereas it is only seen at the lowest θ_{Cu} studied on the 540-K samples. The difference in the dispersion of Cu at the surface of the two series leads us to suggest that this state arises from CO attached to "single" Cu atoms.

If the Cu coverage in the 1080-K series is increased beyond $y = 0.25$ ($\theta_{Cu} \sim 0.3$) a new state becomes apparent—α_2. At the same time the α_1 state also appears. These two states have opposite work function effects. The α_1 causing a work function increase and the α_2 a decrease. The change from a negative $\Delta\varphi$ to a positive $\Delta\varphi$ observed as the α_2 state first fills followed by the α_1 state seems to be in line with the similar behaviour observed as a function of CO coverage on bulk Cu(111). We therefore associate these states with the development of Cu clusters and ultimately bulk copper. In accordance with our other evidence for the early development of Cu clusters these states begin to appear at a lower θ_{Cu} on the 540-K series. With regard to the behavior of the "bulk" Cu films, a word has to be said about the position of the CO desorption maxima on the temperature scale. Clearly both our α_1 and α_2 "Cu" desorption states appear at too high a temperature as compared to the CO desorption features obtained with bulk Cu(111) single-crystal surfaces (*9, 10*). Besides pumping-off effects we tentatively explain the shift ΔT, of ~20–40 K toward higher temperatures as being caused by structural imperfections in our films which may provide sites with higher CO binding energy.

In the θ_{Cu} region 0.15–0.70 in the 1080-K series, a new adsorption state (α_4) is evident in the $d\Delta\varphi/dT$ "spectrum." It is accompanied by a positive work function change and T_{max} is about 310 K. It is evidently associated with Cu, probably Cu clusters, but the positive $\Delta\varphi$ and high desorption temperature suggest the involvement of Ru. We therefore suggest that this site is associated with "mixed" Cu–Ru sites probably occurring around the periphery of Cu clusters. Again, in agreement with this suggestion these sites are observed at lower θ_{Cu} on the 540-K series.

The observation of the strikingly increased CO adsorption capacity in the range around $\theta_{Cu} \sim 0.1$ with the first appearance of the α_3 state supports the conclusion that isolated dispersed Cu atoms not only provide more than just one CO adsorption site but also create "mixed" sites by electronic interaction with adjacent Ru atoms.

4. DISCUSSION AND CONCLUSIONS

The structural, electronic, and energetic properties of the bimetallic Cu/Ru surfaces as used in the present study have been investigated separately (*1, 2, 21*). The features pertinent for the present investigation will first be briefly summarized in order to provide a basis for the discussion of the CO adsorption results: The heat of adsorption of Cu on a Ru(0001) surface exceeds the sublimation enthalpy of bulk copper by a few kilocalories per mole (*2*). As a consequence Cu tends to spread over the Ru surface in the submonolayer range rather than to form small three-dimensional Cu crystallites. The existence of lateral attractive interactions between chemisorbed Cu atoms leads to a tendency for two-dimensional island formation. Work function measurements indicate a small "extra" transfer of electronic charge from Ru to Cu. As a consequence not only the electronic properties of the chemisorbed Cu atoms in the first monolayer will be different from those of bulk copper, but we also expect a slight modification of the electronic properties of those surface Ru atoms which are in the vicinity of a chemisorbed Cu atom. The observed influence of the temperature of preparation on the CO adsorption properties suggests that the structural properties of both series of samples were somewhat different which has to be ascribed to nonequilibrium effects: The samples prepared at a substrate temperature of 1080 K were rapidly cooled down (with a rate of about 100 K/sec) so that the high-temperature

equilibrium structure will at least be partly frozen in. Under these conditions, at small Cu concentrations, the attractive interaction energy between neighboring Cu atoms will be overcome the thermal energy kT so that a fairly high concentration of isolated and randomly distributed Cu atoms is expected. Increasing the Cu coverage will then lead to the formation of oligomers and of larger islands first restricted to the first monolayer.

The situation is certainly quite different for the 540-K series: The tendency for two-dimensional clustering will prevail, but due to the restricted surface mobility also the possibility for the formation of three-dimensional Cu particles exists already at total surface concentrations below that for a complete monolayer.

Based on all the structural information which is available for metallic overlayers (*37*) we may safely assume that the isolated Cu atoms are located in sites with highest coordination, i.e., the threefold sites of the Ru(0001) surface.

When considering the present results for CO adsorption on pure Ru(0001) and Cu(111) there is generally quite good agreement with previous data reported in the literature for both systems (*7, 10, 29–31*) with one major exception: The initial sticking coefficient for CO on Ru(0001) was found to be substantially lower than the value of about 0.5 reported by Menzel *et al.* (*7, 31*). Even if the uncertainty in the pressure gauge calibration is taken into account the data of Fig. 1 clearly indicate that s_0 is far below unity, a value approximately found with many other CO/metal systems. This point will be of some importance for the discussion of the adsorption kinetics at the bimetallic surfaces.

The results with the Cu/Ru surfaces can be rationalized on the basis of concepts developed for chemisorption and catalysis on alloy surfaces. In this connection Sachtler (*18*) introduced the terms "ligand" and "ensemble" effects:

The "ligand" effect comprises the fact that electronic interactions between the constituents modify their chemisorptive properties. In contrast to older views this is certainly a localized phenomenon since deviations from charge neutrality are rapidly screened in a metal. In the present context this means first that the adsorptive properties of Ru atoms adjacent to a Cu atom might be modified. It has been mentioned above that deposition of Cu onto Ru causes transfer of electronic charge from Ru to Cu. According to the generally accepted picture on the mechanism of CO chemisorption (*38*), a substantial contribution to the bond formation arises from "back-donation" of electron charge from the metal to the empty $2\pi^*$ level of the ligand. This effect is also responsible for the negative dipole moment of the adsorbate complex as manifested by the increase of the work function observed with most transition metals. (Cu has a low-lying d band and therefore this effect is almost missing. As a consequence the adsorption energy is much lower than, say, on Ni or Ru, and the work function change has the reverse sign). Based on this model it is predicted that both the adsorption energy and the dipole moment of CO adsorbed on Ru sites in the vicinity of Cu atoms would be smaller than on a pure Ru surface. This agrees exactly with the present observations: A small decrease of the average adsorption energy of the β_3 state by about 7 kJ/mole was derived from the TDS results, whereas the isosteric heat measurements indicated a somewhat stronger decrease by about 20 kJ/mole. Roughly speaking, the variation of the adsorption energy on Ru sites by the presence of adjacent Cu atoms is about one order of magnitude smaller than the adsorption energy itself. It should be noted that similar observations on a small decrease of the adsorption energy were previously made for H_2 on Ru sites of Cu/Ru surfaces (*3*), as well as for CO on Ni sites of Cu/Ni surfaces (*15*).

Much more pronounced is the influence on the dipole moment of the adsorbed complex which is strongly decreased by the

addition of Cu (cf. Fig. 4). Interestingly the value for pure Ru is again attained at higher Cu concentrations. This parallels qualitatively the observations (*1, 2*) that the Cu-induced work function increase passes through a maximum.

The influence of electronic interactions on the adsorption of CO at Cu sites is not so clearly evident: It was experimentally not possible to attain low enough temperatures which enabled complete saturation of the CO adlayer on the pure Cu(111) surface. Nevertheless the thermal desorption and particularly the $d\Delta\varphi/dT$ data may indicate an increase of the adsorption energy on pure Cu sites existing as either single atoms or small clusters, as compared to sites on a continuous Cu(111) overlayer. This is in agreement with corresponding observations made by Yu *et al.* (*15*) with Cu/Ni alloy surfaces.

Much more pronounced is the influence of the so-called "ensemble" effect. This comprises the fact that the chemisorption bond involves not only a single surface atom but rather a group of neighboring atoms. The observed reduction of the amount of strongly (i.e., on pure Ru sites) adsorbed CO with Cu concentration suggested that about three neighboring Ru atoms are involved in this bond formation. Quite similar numbers were derived previously for CO adsorption on other bimetallic (alloy) surfaces. However, the situation is certainly not so simple: There is evidence that even isolated Ru atoms may strongly adsorb CO in a terminal configuration. Support for this view is obtained from ir work with Ag/Pd alloys by Sachtler *et al.* (*39*) which demonstrated that addition of Ag decreased the population of "bridge"-bonded CO but even increased that with a linear bond. Another aspect in this connection concerns the creation of "mixed" sites, where the CO molecule is attached to a group of surface atoms consisting of both Cu and Ru. The adsorption energy on these sites (e.g., α_4) is between that on pure Cu or pure Ru sites as becomes clearly evident from the thermal desorption and the $d\Delta\varphi/dT$ data. Again the work by Yu et al. (*15*) has to be mentioned in this context, where with Cu/Ni alloys similar additional desorption maxima were observed. Since at a given Cu concentration the Cu atoms are not regularly dispersed over the surface in general a whole spectrum of surface atom configurations is expected which should give rise to a rather continuous variation of the adsorption energy, which causes the large observed widths of the desorption features.

Perhaps the most surprising result was the observed pronounced increase of the totally adsorbable amount of CO at small Cu concentrations. Although the microscopic surface area is increasing due to "roughening" this cannot account for the full effect. One has rather to speculate that the isolated Cu atoms on top of the Ru surface are able to bind perhaps two CO molecules. Our data here suggests that small surface clusters are even more efficient in this than single atoms since the increase in θ_{CO} around $\theta_{Cu} = 0.1$ is even more pronounced in the 540-K series. This view is supported by infrared investigations with small Rh particles where also on the existence of $Rh(CO)_2$ species was concluded (*22*) as well as by the existence of matrix-isolated carbonyls like $Cu(CO)_2$ or $Cu(CO)_3$ (*23*). It would be quite interesting to investigate this problem further by means of vibrational spectroscopic techniques.

Another point of discussion concerns the adsorption kinetics: It was found that the initial sticking coefficient on Ru sites, s_0, is markedly increased by the addition of Cu. This quantity is remarkably small for Ru(0001), whereas a value near unity is expected for Cu. Cu atoms on the surface may then be considered as sites where incoming CO molecules are captured with high probability in a weakly held state from where they can "spill-over" to Ru sites prior to desorption. With increasing Cu concentration the mean diffusion path be-

comes longer and therefore the probability for desorption increases—the sticking coefficient drops again. The increase of the sticking coefficient with CO coverage on pure Ru would then have a quite similar origin: Here the preadsorbed CO molecules offer such a "precursor" state.

Finally a short qualitative comparison of the behavior of the so far investigated gases (H_2, O_2, N_2O, CO) interacting with single crystalline Cu/Ru systems will be made:

(i) The most pronounced effects are found with H_2. The dissociation probability of this molecule is fairly high on Ru and very small on Cu. In addition, the Cu–H bond is rather weak. It was concluded that fairly large "ensembles" of Ru atoms are needed for dissociative chemisorption of this molecule. As a consequence both the sticking coefficient and the saturation density of strongly held hydrogen atoms is sharply reduced by the addition of small amounts of copper (*3*). Therefore also catalytic reactions involving chemisorbed hydrogen atoms (e.g., hydrogenolysis of saturated hydrocarbons) will also be strongly inhibited (*5*).

(ii) O_2 adsorbs dissociatively on Ru and (with somewhat smaller probability) on Cu and is also strongly bound to both metals. As a consequence no pronounced influence of the addition of Cu atoms was found with this system (*4*).

(iii) N_2O reacts dissociatively (to N_2 + O_{ad}) with both Ru(0001) and Cu surfaces. Whereas the reaction probability is rather high with Ru it is much smaller on Cu surfaces. As a consequence the total uptake is only slightly influenced by Cu, whereas on the other hand the reaction probability is drastically lowered by the addition of Cu atoms. Obviously again (as in the case of hydrogen) a fairly large ensemble of adjacent Ru atoms is needed for the high reactivity (*4*).

(iv) CO adsorbs nondissociatively: The ensemble effect is less pronounced, i.e., a Cu atom blocks only about three Ru sites, and the sticking coefficient is at first even increasing since the Cu atoms may provide a "precursor" state with a high probability for accommodation of the incoming CO molecule. A more or less continuous variation of the CO adsorption energy between the values for pure Cu and pure Ru is provided due to the existence of "mixed" Cu + Ru adsorption sites. In addition, a marked increase of the saturation concentration of weakly held CO is observed at low Cu concentrations, since an isolated Cu atom on top of the Ru surface may presumably bind more than one CO molecule.

It is felt that the trends just outlined will also hold for other molecules, i.e., depending on their kind (dissociative or nondissociative), kinetics and strength of interaction. With the pure constituents, a more or less dramatic variation of the reactivity and saturation coverage will occur. This provides some idea on possible variations of the selectivity of steady-state reactions taking place at bimetallic catalysts.

ACKNOWLEDGMENTS

This work has been made possible by financial support from the Deutsche Forschungsgemeinschaft (SFB 128). One of us (JCV) gratefully acknowledges support by the Alexander-von-Humboldt Foundation, and the Science Research Council.

REFERENCES

1. Christmann, K., Ertl, G., and Shimizu, H., *Thin Solid Films* **57**, 247 (1979).
2. Christmann, K., Ertl, G., and Shimizu, H., *J. Catal.* **61**, 397 (1980).
3. Shimizu, H., Christmann, K., and Ertl, G., *J. Catal.* **61**, 412 (1980).
4. Shi, S. K., Lee, H. I., and White, J. M., *Surface Sci.* **102**, 56 (1981).
5. Sinfelt, J. H., Lam, Y. L., Cusamano, J. A., and Barnett, E. A., *J. Catal.* **42**, 227 (1976).
6. Sinfelt, J. H., *Chem. Eng. News* **50**, 18 (1972); *Acc. Chem. Res.* **10**, 15 (1977).
7. Madey, T. E., and Menzel, D., "Proc. 2nd Intern. Conf. Solid Surfaces, 1974," *Japan. J. Appl. Phys. Suppl.* **2**, 229 (1974).
8. Williams, E. D., and Weinberg, W. H., *Surface Sci.* **82**, 93 (1979).
9. Hollins, P., and Pritchard, J., *Surface Sci.* **89**, 486 (1979).
10. Hollins, P., and Pritchard, J., *Surface Sci.* **99**, L389 (1980).

11. Vannice, M. A., *J. Catal.* **37,** 449, 462 (1975).
12. Dalla Betta, R. A., Piken, A. G., and Shelef, M., *J. Catal.* **35,** 54 (1974).
13. Bond, G. C., and Turnham, B. D., *J. Catal.* **45,** 128 (1976).
14. Bossi, A., Carnisio, G., Garbassi, F., Griunchi, G., Petrini, G., and Zanderighi, L., *J. Catal.* **65,** 16 (1980).
15. Yu, K. Y., Ling, D. T., and Spicer, W. E., *J. Catal.* **44,** 373 (1973).
16. Burton, J. J., Helms, C. R., and Polizzotti, R. S., *J. Chem. Phys.* **65,** 1089 (1976).
17. Ertl, G., *in* "The Nature of the Surface Chemical Bond" (T. N. Rhodin and G. Ertl, Eds.), North-Holland, Amsterdam/New York, 1979.
18. Sachtler, W. M. H., *Le Vide* **164,** 67 (1973).
19. Balandin, A. A., *Zh. Russ. Fiz. Khim. O. Chast Khim.* **61,** 909 (1929); *Z. Phys. Chem. B* **2,** 289 (1929).
20. Balandin, A. A., *in* "Advances in Catalysis and Related Subjects" (D. D. Eley, H. Pines, and P. B. Weisz, Eds.), Vol. 19, p. 1. Academic Press, New York, 1969.
21. Christmann, K., Heimann, P., Vickerman, J. C., Ertl, G., Himpsel, F. J., and Eastman, D. E., in preparation.
22. Yates, J. T., Jr., Duncan, T. M., Worley, S. D., and Vaughan, R. W., *J. Chem. Phys.* **70,** 1219 (1979).
23. Huber, H., Kündig, E. P., Moskovits, M., and Ozin, G. A., *J. Amer. Chem. Soc.* **97,** 2097 (1975).
24. Conrad, H., Herz, H., and Küppers, J., *J. Phys. E* **12,** 369 (1979).
25. Madey, T. E., Engelhardt, H. A., and Menzel, D., *Surface Sci.* **48,** 304 (1975).
26. Goodman, D. W., and White, J. M., *Surface Sci.* **90,** 201 (1979).
27. Christmann, K., and Ertl, G., *Thin Solid Films* **28,** 3 (1975).
28. Prestridge, E. B., Via, G. H., and Sinfelt, J. H., *J. Catal.* **50,** 115 (1977).
29. Menzel, D., *J. Vac. Sci. Technol.* **12,** 313 (1975). Fuggle, J. C., Madey, T. E., Steinkilberg, M., and Menzel, D., *Phys. Lett. A* **51,** 163 (1975).
30. Pfnür, H., Feulner, P., Engelhardt, H. A., and Menzel, D., *Chem. Phys. Lett.* **59,** 481 (1978).
31. Fuggle, J. C., Madey, T. E., Steinkilberg, M., and Menzel, D., *Surface Sci.* **52,** 521 (1975).
32. Pritchard, J., Catterick, T., and Gupta, R. K., *Surface Sci.* **53,** 1 (1975); Pritchard, J., *J. Vac. Sci. Technol.* **9,** 895 (1972); Pritchard, J., *Surface Sci.* **79,** 231 (1979).
33. Redhead, P. A., *Vacuum* **12,** 203 (1963).
34. Chan, C. M., Aris, R., and Weinberg, W. H., *Appl. Surf. Sci.* **1,** 360 (1978).
35. Tracy, J. C., and Palmberg, P. W., *J. Chem. Phys.* **51,** 4852 (1969).
36. Engelhardt, H. A., Feulner, P., Pfnür, H., and Menzel, D., *J. Phys. E* **10,** 1133 (1977).
37. van Hove, M. A., *in* "The Nature of the Surface Chemical Bond" (T. N. Rhodin and G. Ertl, Eds.), North-Holland, Amsterdam, 1979.
38. Blyholder, G., *J. Chem. Phys.* **68,** 2772 (1964); Doyen, G., and Ertl, G., *Surf. Sci.* **43,** 197 (1974).
39. Soma-Noto, Y., and Sachtler, W. M. H., *J. Catal.* **32,** 315 (1974).